Hindawi
Geofluids
Volume 2022, Article ID 1304176, 15 pages
https://doi.org/10.1155/2022/1304176

Research Article

Modeling and Dynamic Performance Analysis of Hydraulic Top Drive Main Transmission System with Long Hydraulic Pipelines

Yuanling Shi and Pingsong Zhang

School of Earth & Environment, Anhui University of Science & Technology, Huainan 232001, China

Correspondence should be addressed to Yuanling Shi; ylshi@aust.edu.cn

Received 1 December 2021; Accepted 29 March 2022; Published 16 April 2022

Academic Editor: Shijin Li

Hydraulic top drive is the main power component used to drive drilling tools rotating to drill a hole for drilling rigs. Its main transmission system was built with hydraulic power source and hydraulic actuators. During the drilling procession, the hydraulic top drive is mounted on a derrick, and moving along its vertical guide rails. The hydraulic power station is usually placed on the drilling platform or the ground. In that way, long pipelines are needed to connect the hydraulic pumps and hydraulic motors. Thus, the effects on the performance of hydraulic top drive should not be neglected. A mathematical model of hydraulic top drive main transmission with differential equation of hydraulic units and state space equation of hydraulic long pipelines was deduced in this research. A simulation model was built using the AMESim software. And field drilling test of the hydraulic top drive was carried out in Songliao Basin Drilling Project (SK-II) well site. To verify and modify the virtual model, a comparison analysis was performed by setting the parameters and load of the three methods at the same values. The result of comparison shows that the simulation results are very close to the theoretical results and field drilling test data. Thus, the dynamic characteristics could be analyzed by this simulation model. Dynamic characteristics of the hydraulic top drive with different length and various diameters of pipelines were studied. The simulation results demonstrate that pipeline lengths and pipeline diameters affect the system in different laws, and it needs to comprehensively consider the system response speed, overshoot, and steady-state characteristics when choosing the size of pipelines for hydraulic top drive.

1. Introduction

Top drive is the main power component used to drive drilling tools rotating on the drilling rigs [1, 2]. Compared with the oil and gas drilling rigs, most of the rigs for geological exploration have not been equipped with top drive, the automation of which needs to be improved urgently. The top drive system drives drilling tools rotating and penetrating rocks, while it travels along its vertical guide rails up and down. According to the power supply, the widely used top drive at present mainly includes electric top drive and hydraulic top drive. In hydraulic top drive, hydraulic power components and hydraulic actuators are used to construct the main transmission system. Electro-hydraulic control technology is usually applied to regulate the output parameters of hydraulic top drive, such as the speed and the torque [3]. Currently, electro-hydraulic system is more and more widely used in industry machine and automation process, whose advantages are glaringly obvious for the occasions requiring fast response speed, high positioning accuracy, and large load. It is mainly because of the convenient speed regulating, great ratio of power to volume, and smooth operation that the electro-hydraulic system can provide, comparing with the DC or AC motors [4–6].

To insure power supply of the hydraulic top drive system, an independent hydraulic power station is often equipped, which can be placed on the drilling floor or on the ground. Considering that the hydraulic top drive moves up and down along its guide rail installed on the derrick, no matter where the hydraulic power station is put, long hydraulic pipelines are needed to connect the hydraulic pumps and hydraulic motors, shown as Figure 1. And the length of hydraulic pipelines can reach to tens of meters, which will lead to the pressure and flow rate inconsistent between hydraulic pumps

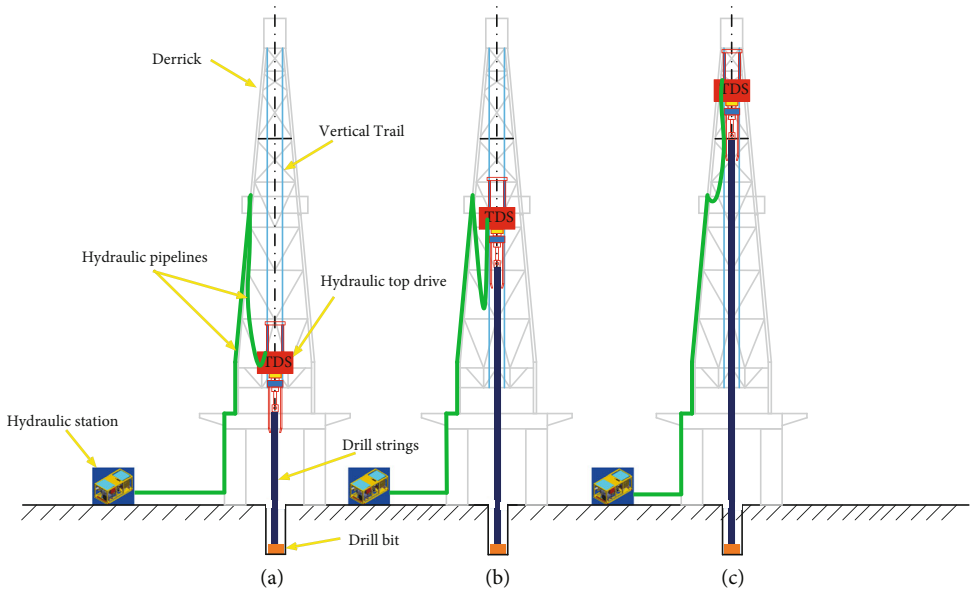

Figure 1: Pipelines form when top drive working. (a) The lowest operation position of hydraulic top drive. (b) The middle operation position of hydraulic top drive. (c) The highest operation position of hydraulic top drive.

and hydraulic motors. In other words, the long hydraulic pipelines have a significant impact on the output performance of top drive. Especially when hydraulic top drive is stopped suddenly or sticking accidents happen during drilling, the load acted on the top drive will change rapidly, which will result in huge pressure shock on hydraulic components, and even result in noise, vibration, and fatigue failure of hydraulic pipelines. Thus, when analyzing the performance of the hydraulic top drive, long hydraulic pipelines should not be neglected.

Analysis of performance and dynamic characteristic of hydraulic system have been investigated by numerous researchers in various fields [7–10], such as the air-craft, construction machinery, and mining mechanics. However, in most of the research, hydraulic pipelines are neglected in modelling and analysis. Since the 1950s, pipeline dynamics have been studied widely [11]. A host of in-depth researches has been done in developing the transient models globally, and both frequency domain model [12] and time domain model [13] have been gained. For investigating the dynamic behaviors of fluid networks [14–17], different modelling approaches, impedance method, transmission line method, and bond graph method for instance, have been found its way. And frequency method, characteristic line method, distributed parameter method, lumped parameter method, etc., are often used in pipeline analysis. N. Nedi'c et al. [18] present a mathematical model with lumped parameters to study a pump-controlled motor system, where the long transmission line is divided into several segments. In literature [19], new bond graphs are put forward by using rational transfer functions and separation of variables techniques, and simulation results with different pipelines are analyzed. In literature [20], bond graph representations for hydraulic pipelines were constructed based on the one-dimensional bond graph structures and modal approximation techniques, and a comparison was made for lossless, 1-D linear fluid friction, and 2-D fluid friction models. In literature [11], a wave energy converter with long pipelines was studied, and transient pressure pulsations and pipelines influence were investigated by using a dynamic model with pipeline modal approximation models [21, 22]. To investigate the dynamic output performance of hydraulic top drive, hydraulic components, such as hydraulic pumps and hydraulic motors, were modeled by means of differential equations. For combining the model of hydraulic components and hydraulic pipelines, the modal approximation model of hydraulic pipelines presented by means of state equation was adopted in this paper.

Due to the advantages, such as convenient modeling, high calculation accuracy, low hardware requirement, and low time consumption, computer simulation analysis is highly applied in various disciplines [23–25]. For a top drive, with high cost of manufacturing, it is a long period from design to application, and field test is not easy to be carried out. It is an economical and efficient technical means for this kind of equipment to build a simulation model, analyzing its performance before manufacturing, predicting faults, and optimizing parameters in the process of application. Based on simulation methods, it will help to improve the design efficiency of top drive, and scan for potential problems comprehensively and accurately without relying on a product. Meanwhile, simulation models can also be used for hydraulic top drive system optimization and drilling parameter selection, during the hydraulic top drive drills as well. Thus, a simulation model will be built in this research in the AMESim software.

This paper is organized as follows: in the second section, the configuration of hydraulic top drive main drive system was introduced, then a mathematical model of which was built with differential equation for hydraulic components and modal approximation model for hydraulic pipelines. In the third section, a simulation model was built using AMESim, and drilling experiment in Songliao Basin Drilling Project (SK-II well site) is described. In the last part of this

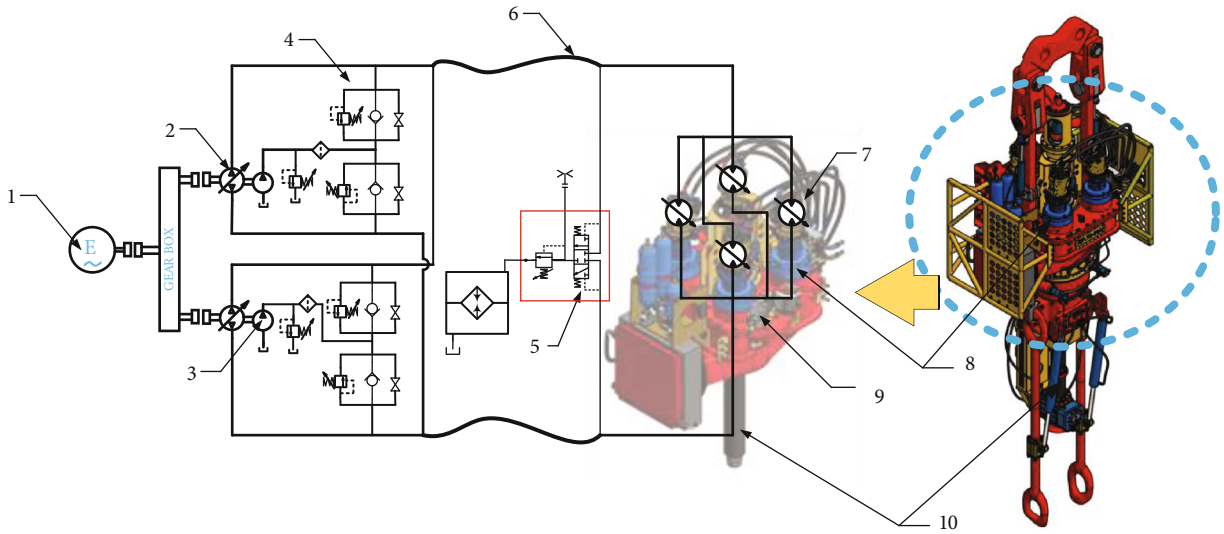

Figure 2: Configuration of top drive main hydraulic system. 1 Prime mover. 2 Variable displacement hydraulic pump. 3 Supplementary circuit. 4 Overload protective circuit. 5 Flush circuit. 6 Long hydraulic pipelines. 7 Variable displacement hydraulic motor. 8 Planetary gearbox. 9 Top drive gear box. 10 Top drive main shaft.

paper, comparative analysis of mathematical results, simulation results, and drilling experiments results is performed, and then dynamic characteristics of hydraulic top drive is investigated with various pipelines considered.

2. Configuration and Mathematical Modelling of the System

2.1. System Configuration. As the hydraulic top drive is mainly used to drive drilling tools rotating, its main transmission system can be regarded as the most important unit, including the main gearbox, hydraulic system, and control system, as shown in Figure 2. For the main gearbox, multi-stage structure is adopted to realize the function of high speed and large torque. During drilling process, the top drive main shaft, mounted in the center of the gearbox, is connected directly with the drill pipe through tread. A large center gear is used to fix the top drive main shaft, outside of which four pinions are engaged. At the top side of each pinion, a small planetary gearbox, a disc brake, and a hydraulic motor are connected sequentially. The disc brakes are used for braking, and planetary gearboxes are used for slowdown and increase torsion. The hydraulic motors provide power to the top drive for rotating.

For the hydraulic system, two hydraulic variable displacement pumps are selected as the power units, and four variable hydraulic displacement motors are chosen as the actuator units. The hydraulic motors are mounted on the body of top drive, and the hydraulic pumps are placed on the ground in the hydraulic power station. Several sections of hydraulic pipelines are used to connect the motors and pumps. What's more, to ensure the system operation, supplementary circuit, overload protective circuit, flush circuit, and other necessary units are equipped.

Electro-hydraulic proportional control technology is adopted to regulate the speed and torque. The displacements of hydraulic pumps and motors are varied with the pilot hydraulic proportional control mode, with a pressure limiting variable pump offering hydraulic control signals. An electromagnetic proportional pressure relief valve is connected with the variable pump and the variable motor displacement control mechanism. When current signals are input, electromagnetic proportional pressure relief valve converts it into hydraulic signals; thus, the displacement of variable pumps and the displacement of variable motors are adjusted.

Table 1: Main parameter of the hydraulic top drive mathematical model.

Parameters	Value
$D_{p\ \max}$	2.5e-4 m^3/rad
ω_p	50π rad/s
k_{rv}	3/65 bar/mA
a	3±0.5 bar
b	11±0.5 bar
$D_{m\ \max}$	2.5e-4 m^3/rad
C_t	5.0e-12 (m^3/s)/Pa
V_{pm0}	2.53e-2 m^3
β_e	7.0e8 N/$(m^2$/Pa)
J	20 kg•m^2
B_m	0.3 N•m/(rad/s)
c	1000 m/s
ρ	0.85e+3 kg/m^3
ν_0	5.0e-5 m^2/s

2.2. Mathematical Model of Hydraulic Top Drive Main Transmission. A closed loop volumetric speed regulation system is adopted to control and drive the main gearbox of the hydraulic top drive, which includes two hydraulic variable

pumps and four hydraulic variable motors. When the mathematical model is developed, the following hypotheses are made.

(1) In order to simplify the model, the two hydraulic pumps are combined into one, and the four hydraulic motors are equivalent to one

(2) The moment of inertia of top drive main shaft is regarded as a constant value

(3) The leakage of hydraulic pump and hydraulic motor remains unchanged, and the leakage mode is laminar flow leakage

(4) The input speed of hydraulic pumps remains unchanged

(5) The pressure on the low pressure side of the system remains constant, thus ignoring the dynamic fluctuation of the pressure at this side

(6) Only the high side pressure is determined by loads

2.2.1. Hydraulic Pump Model. Two axial piston variable pumps are adopted in the hydraulic top drive, and the input speed remains constant. The flow rate outflowing from the hydraulic pumps is equal to that incoming the hydraulic pipelines. Flow equation of the hydraulic pump is as follows:

$$Q_1 = D_p\omega_p - C_{ip}(P_1 - P_c) - C_{ep}P_1 - \frac{V_p}{\beta_e}\dot{P}_1, \tag{1}$$

where Q_1 is the flow rate of the pump, D_p is the displacement of the pump, m^3/rad; ω_p is the angular velocity of the pump, rad/s; P_1 is the outlet pressure of the hydraulic pump, Pa; P_c is the supplementary pressure, Pa; C_{ip} is the internal leakage coefficient of the pump, $(m^3/s)/Pa$; and C_{ep} is the external leakage coefficient of the pump, $(m^3/s)/Pa$.

2.2.2. Hydraulic Motor Model. Four axial piston variable motors are applied in the hydraulic top drive. And the flow rate flowing into the hydraulic motors is equal to that flowing out of the hydraulic pipelines. The flow equation of the variable displacement hydraulic motor is as follows:

$$Q_2 - C_{im}(P_2 - P_c) - C_{em}P_2 = D_m\omega_m + \frac{V_m}{\beta_e}\dot{P}_2, \tag{2}$$

where Q_2 is the flow rate flowing into hydraulic motor; P_2 is the inlet pressure of hydraulic motor, Pa; C_{im} is the internal leakage coefficient of the motor, $(m^3/s)/Pa$; C_{em} is the external leakage coefficient of the motor, $(m^3/s)/Pa$; D_m is the motor displacement, m^3/rad; ω_m is the angular velocity of the motor, rad/s; V_m is the average volume of the hydraulic motor, m^3; and β_e is the effective bulk modulus of the system, $N/(m^2/Pa)$.

The torque on the hydraulic motor is balanced, and the balance equation is

$$T_g = D_m(P_2 - P_c) = J\dot{\omega}_m + B_m\omega_m + T_L, \tag{3}$$

where T_g is the theory torque on the motor, N•m; J is the total inertia of the motor, $kg•m^2$; B_m is the vicious damping coefficient, N•m/(rad/s); and T_L is the load torque, N•m.

2.2.3. Mathematic Model of Long Hydraulic Pipelines. Regarding the fluid transmission line as a distributed parameter system, an accurate model of it is established [26, 27]. There are four possible sets of boundary conditions for the one-dimensional distributed parameter model of the fluid transmission line, and each boundary condition corresponds to an input-output configuration. The above four possible boundary condition configurations are $[P_{up}, P_{down}]$, $[Q_{up}, Q_{down}]$, $[P_{up}, Q_{down}]$, or $[P_{down}, Q_{up}]$ as inputs, respectively. Generally, when both ends of the pipelines are connected to valves, the flow rate inputs model $[Q_{down}, Q_{up}]$ will be applied, while when both ends of the pipelines are connected to volumes, the pressure inputs model $[P_{up}, P_{down}]$ is usually adopted. Considering that for the hydraulic top drive, long pipelines are connected to hydraulic pumps and hydraulic motors, which all can be regarded as volumes, the pressure inputs model is applied in this paper. The hydraulic pipelines model is expressed as follows:

$$\begin{bmatrix} Q_1 \\ Q_2 \end{bmatrix} = \begin{bmatrix} \dfrac{\cosh \Gamma(s)}{Z_c(s)\sinh \Gamma(s)} & -\dfrac{1}{Z_c(s)\sinh \Gamma(s)} \\ \dfrac{1}{Z_c(s)\sinh \Gamma(s)} & -\dfrac{\cosh \Gamma(s)}{Z_c(s)\sinh \Gamma(s)} \end{bmatrix} \begin{bmatrix} P_1 \\ P_2 \end{bmatrix}, \tag{4}$$

where P_1 and P_2 are the upstream pressure and downstream pressure of the pipelines, respectively; and Q_1 and Q_2 are the upstream flow rate and downstream flow rate, respectively.

The fluid performance in transmission line is dominated by the characteristic impedance Z_c and the propagation operator $\Gamma(s)$. Because there are several basic model for pipelines, such as the lossless model, the linear friction model, and the dissipative model, the expressions for the line characteristic impedance and the propagation operator is different when different basic model is selected. For the linear friction model, these two parameters are defined as follows:

$$\begin{aligned} \Gamma(\bar{s}) &= D_n\bar{s}\left[1 + 8/\bar{s}\right]^{1/2}, \\ Z_c(\bar{s}) &= Z_0\left[1 + 8/\bar{s}\right]^{1/2}, \end{aligned} \tag{5}$$

where $\bar{s}$ is the normalized Laplace operator, which is given as $\bar{s} = s/\omega_c$; ω_c is the viscosity frequency, which is given as $\omega_c = \nu_0/r^2$; r_h is the inner radius of the pipe; D_n is the dissipation

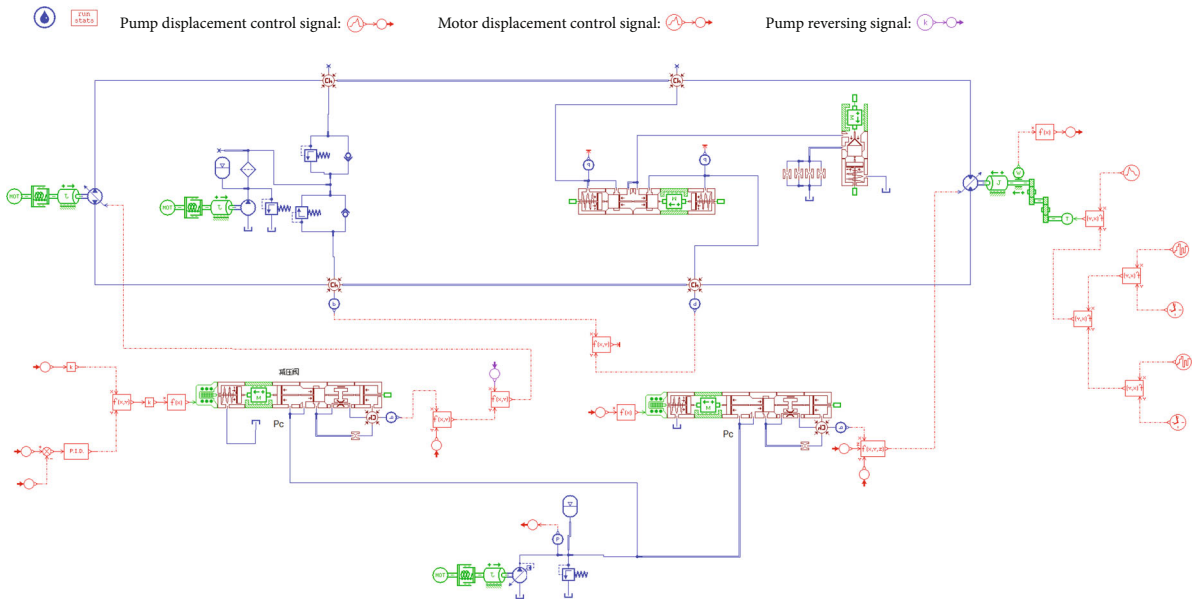

Figure 3: Simulation model of hydraulic top drive with long pipelines.

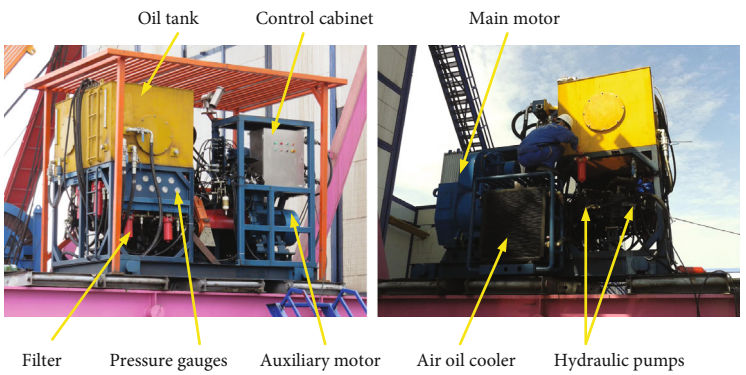

Figure 4: Hydraulic power station of the top drive.

Table 2: Hydraulic units information of the top drive.

Element	Type	Maker	Quantity
Hydraulic piston pump	90-R250-HF	SAUER-DANFOSS	2
Hydraulic piston motor	51 V250-A-F2-N-HS	SAUER-DANFOSS	4
Pressure-limited variable pump	LRR-030-DPC	SAUER-DANFOSS	1
Pressure reducing valve	EHPR98-T38-0-N-24ER	HYDRA-FORCE	2
Incremental encoder	BEI-HS35F-100	BEI-SENSOR	1
Hydraulic pipeline	F38VI	EATON	80 m

number; and Z_0 is the line impedance constant. The last two parameters are defined as follows:

$$D_n = \frac{l\nu_0}{cr^2}, \qquad Z_0 = \frac{\rho c}{A_p}, \tag{6}$$

where l is the length of the pipelines; ν_0 is the kinematic viscosity of the working fluid; c is the acoustic velocity, which is

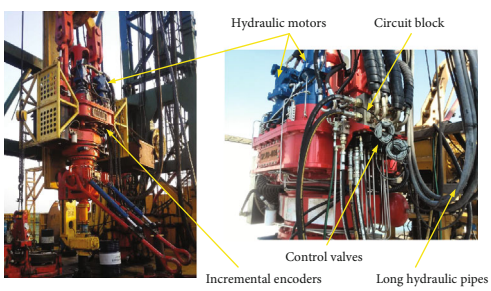

Figure 5: Hydraulic top drive in drilling experiment.

Table 3: Pipeline configuration of the top drive.

Pipeline section	Length/mm	Inner diameter/mm
Pump A and B to circuit block	500	25.4
Circuit block to HYDAC filter	500	25.4
HYDAC filter to drill floor circuit block	2000	25.4
Drill floor circuit block to derrick circuit block	2500	25.4
Derrick circuit block to top drive motor	2400	25.4

defined as $c = \sqrt{\beta_e/\rho}$; β_e is the effective bulk modulus of working fluid; ρ is the density of the oil; and A_p is the cross-sectional area of the pipe.

Considering that the hydraulic system of the top drive is a nonlinear system, it cannot be easy to calculate and analyze in frequency domain. To integrate the hydraulic pump model, hydraulic motors model, and hydraulic pipeline model, an approximate model of hydraulic pipelines proposed in the literature [11, 20, 22] is adopted in this paper. The approximate model can be regarded as a finite dimensional state space model:

$$\begin{aligned} \frac{1}{\omega_c}\dot{\mathbf{X}} &= \mathbf{AX} + \boldsymbol{Bu}, \\ \mathbf{Y} &= \mathbf{CX}, \end{aligned} \tag{7}$$

where

$$\begin{aligned} \mathbf{X} &= [Q_{10}Q_{20}\, Q_{11}Q_{21} \cdots Q_{1n}Q_{2n}]^T, \\ \boldsymbol{u} &= [P_1 P_2]^T, \\ \mathbf{Y} &= [Q_1 Q_2]^T, \\ \mathbf{A} &= \text{diag}\,[A_0, A_1, \cdots, A_n], \\ \mathbf{B} &= [B_0, B_1, \cdots, B_n]^T, \\ \mathbf{C} &= [I_0, I_1, \cdots, I_n], \end{aligned} \tag{8}$$

with

$$\begin{aligned} \boldsymbol{A}_0 &= \begin{bmatrix} -8 & 0 \\ 0 & -8 \end{bmatrix}, \boldsymbol{B}_0 = \frac{1}{Z_0 D_n}\begin{bmatrix} 1 & -1 \\ 1 & -1 \end{bmatrix}, \mathbf{I}_0 = \begin{bmatrix} 1 & 0 \\ 0 & 1 \end{bmatrix}, \\ \boldsymbol{A}_i &= \begin{bmatrix} 0 & -\lambda_{si}^2 \\ 1 & -8 \end{bmatrix}, \boldsymbol{B}_i = \frac{2}{Z_0 D_n}\begin{bmatrix} 0 & 0 \\ 1 & -(-1)^i \end{bmatrix}, \boldsymbol{I}_i = \begin{bmatrix} 0 & 1 \\ 0 & (-1)^i \end{bmatrix}, \end{aligned} \tag{9}$$

where $i = 1, 2, 3 \cdots, n$; λ_{si} is root indices, which is defined as $\lambda_{si} = \pi i/D_n$. Other parameters are defined as above.

Table 1 shows the values of the above mathematical model parameters for the top drive hydraulic system.

3. Simulation Model and Field Test

3.1. Simulation Model. In Section 2, the mathematical model of hydraulic top drive has been established, which contains a series of differential equations. Based on the above model, it is difficult to obtain the analytical solution and analyze the dynamic characteristics of the system under different conditions. To analyze the dynamic characteristics of the hydraulic top drive with long pipelines, a simulation model is built in AMESim platform, shown as Figure 3. The hydraulic system of the top drive includes two parallel hydraulic pumps, which drive four parallel hydraulic motors. For a simulation model, setting the number of hydraulic pumps and motors according to the real configuration of the hydraulic top drive will lead to the simulation model jumbled and complex, not conducive to debugging and calculation. Thus, on the premise of not affecting the simulation results, the two hydraulic pumps and four hydraulic motors are equivalent to one pump and one motor, respectively, in the simulation model, to simplify model and improve calculation speed. The maximum displacement of the hydraulic pump in simulation model is the sum of the maximum displacement of the two hydraulic pumps in the real configuration system, and so is the hydraulic motor. So, the simulation model contains a hydraulic pump and its variable displacement mechanism, a hydraulic motor and its variable displacement mechanism, long hydraulic pipelines, supplementary circuit, overload

Figure 6: Cores obtained by the hydraulic top drive.

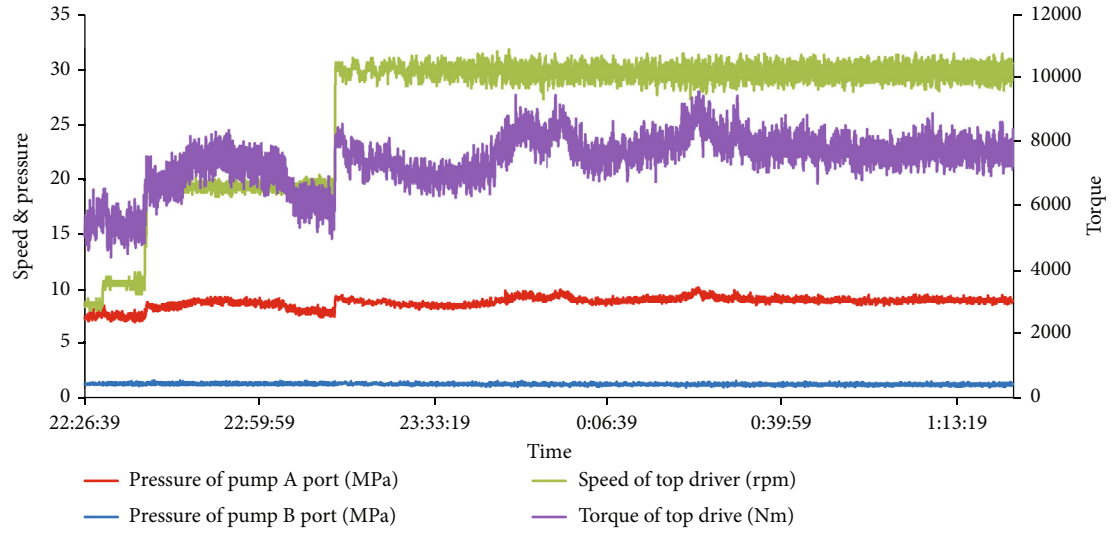

Figure 7: Experiment data when top drive drilling in SK-II at the depths of 3436.92 m to 3447.52 m.

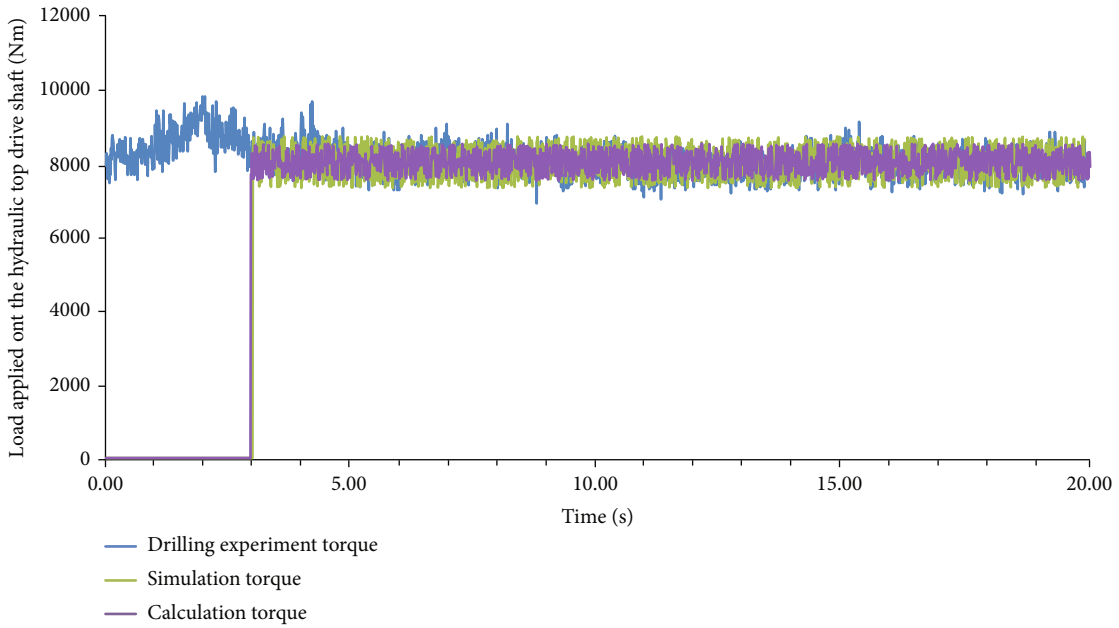

Figure 8: Loads applied on the hydraulic top drive.

protective circuit, flush circuit, loading part, top drive gear transmission part, control signals, and other necessary parts.

3.2. Field Test. Thanks to the deep continental scientific drilling project, field test of the top drive was carried out in Songliao Basin Drilling Project well site. As one of the key automation devices of the CRUST-I 10000m scientific drilling rig, the hydraulic top drive drove drilling tools to cutting rocks while travelling along a special guide mounted in the derrick of the rig. The hydraulic power station was placed on the ground, shown in Figure 4. The hydraulic components, such as prime motor, hydraulic pumps, hydraulic oil tank, control cabinet, and hydraulic valves, are included in the power station. Table 2 lists the type and quantity of hydraulic units of the top drive. Figure 5 shows the hydraulic top drive in drilling experiment. The hydraulic motors and several control valves were installed on the hydraulic top drive.

There are five sections of hydraulic pipelines used to connect the hydraulic pumps and hydraulic motors. The configuration of the five sections hydraulic pipelines is detailed in Table 3. Eaton's Triple Crown GH493-16 hose is selected to connect the hydraulic pumps and hydraulic motors, whose inner diameter is 25.4 mm, outer diameter is 37.6 mm, maximum operating pressure is 350 bar, and operating temperature is in the range of -40°C to 127°C. For the CRUST-I drilling rig, the height of its derrick is

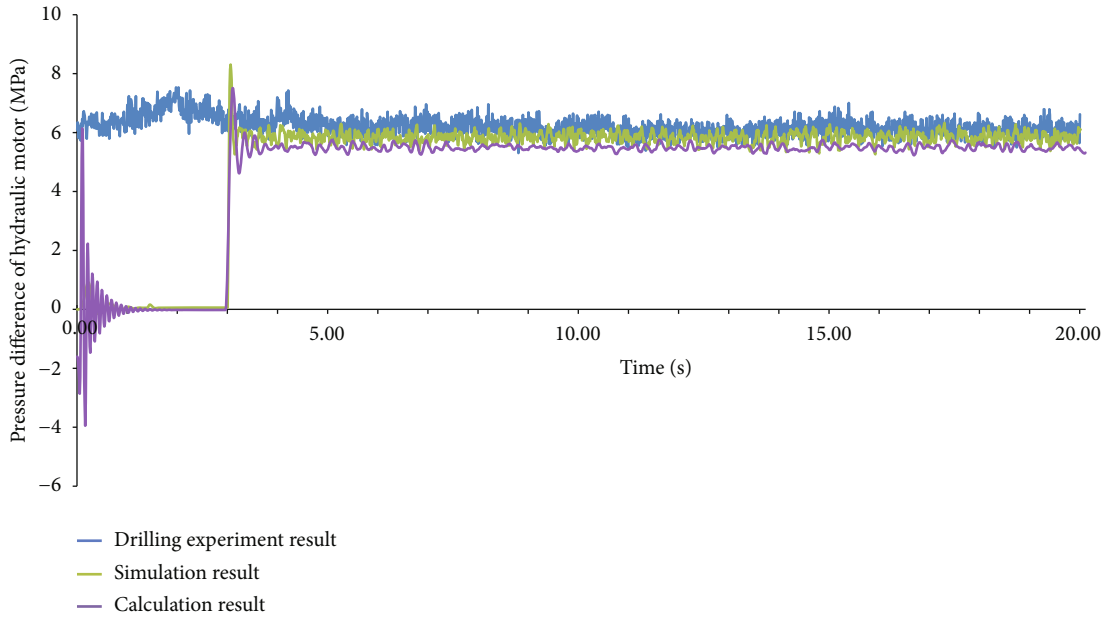

Figure 9: Pressure difference of hydraulic motor.

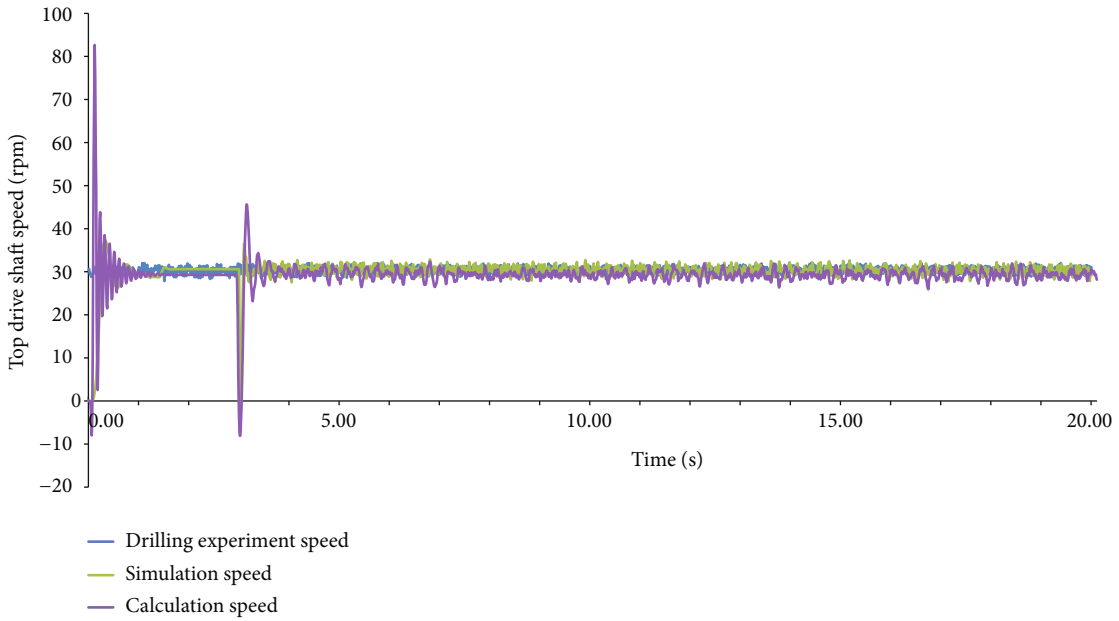

Figure 10: Output speed of the hydraulic top drive.

48 m, and the height of its drilling floor is 12 m. The maximum distance that the hydraulic top drive travels is 36.5 m. Thus, the total length of hydraulic pipelines used in the drilling experiment is 80 m.

The field trail site is located in Anda, Heilongjiang, China. The purpose of the Songliao Basin Drilling Project is to penetrate the Cretaceous continental stratum and get the complete sedimentary records of the whole Cretaceous continental stratum. The design depth of the SK-II well is 6400 m, and finally the well was completed with the depth of 7018 m.

Drilling experiments were implemented in two phases. The first phase was performed from the depth of 2800 m to the depth of 3628 m. During this stage, sweeping borehole was carried out by the top drive from the depth of 2800 m to the depth of 3100 m, and then core drilling was conducted from the depth of 3100 m to the depth of 3628 m. Totally, the hydraulic top drive ran for 66 days, and 28 barrels of core were obtained. Besides, the longest core was obtained with the length of 30.49 m between the depth of 3675.59 m and 3706.08 m, and coring rate reached to 100%. Based on the stratum histogram of the SK-II well, the stratum from 2840 m to 3320 m is Yingcheng Formation, and from 3320 m to 5670 m is Shahezi Formation. The upper part of the Yingcheng Formation is mainly green gray coarse sandstone, conglomerate and glutenite, purple and mottled purple tuff with

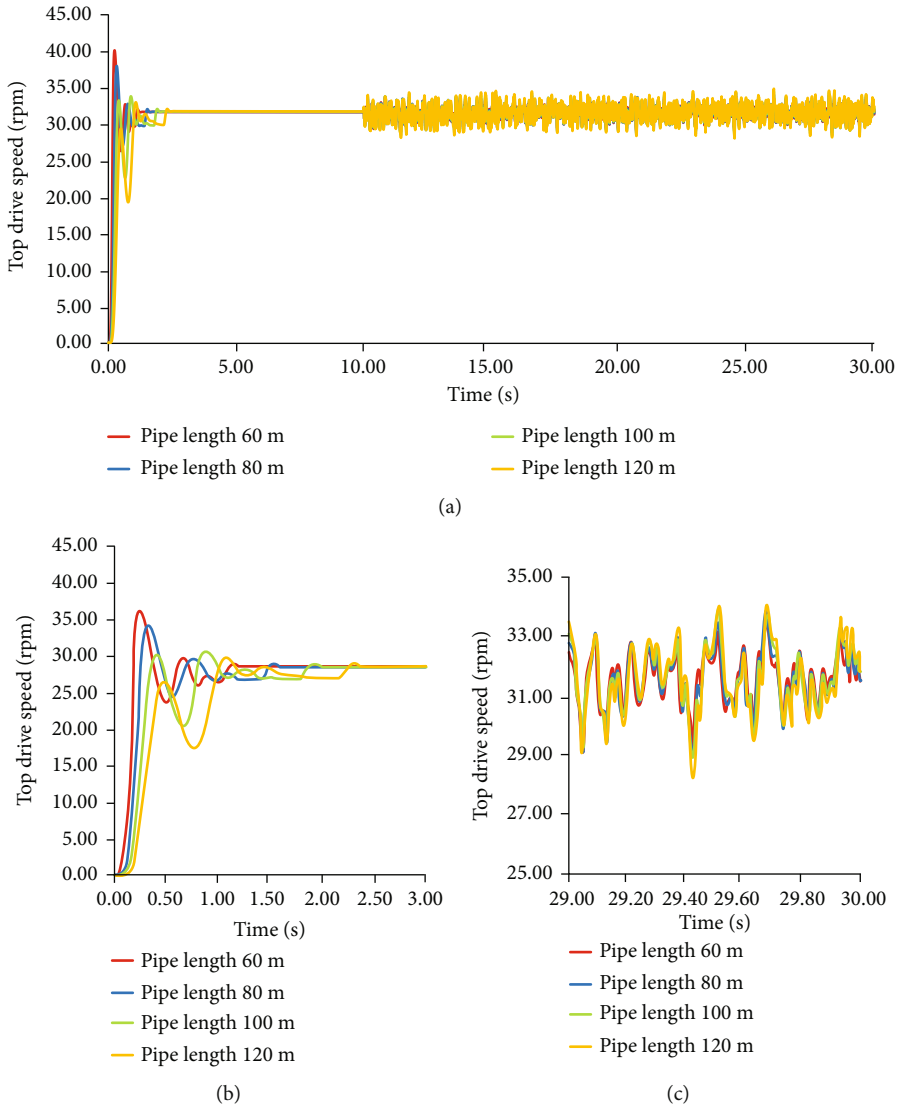

Figure 11: Top drive shaft speed with different pipe length. (a) Speed from the beginning to the 30th second. (b) Speed from the beginning to the 3rd second. (c) Speed from the 29th second to the 30th second.

thin layer of conglomerate, thick mottled and gray conglomerate with thin layer of purple mudstone; the lower part is a very thick layer of tuff, thick layers of green and gray tuff mixed with gray andesite basalt. The Shahezi Formation is mainly composed of black mudstone intercalated with black coal line, intercalated with thin layers of gray fine sandstone, dark gray siltstone and argillaceous siltstone; the bottom is interbedded with gray sandy conglomerate, coarse sandstone and gray black mudstone. Figure 6 shows cores obtained when the hydraulic top drive drilled the hole. The second stage of drilling experiment was carried out from the depth of 6769.77 m to the depth of 7108.88 m. During this period, the hydraulic top drive drilled the cement plug, with totally 5 trips and a total trip of about 62000 m.

4. Result and Discussion

4.1. Comparison of Mathematical Results, Simulation Results, and Experiment Data. During the drilling test, the top drive operated continuously 24 hours a day. All parameters of top drive operation, such as speed, torque, and pressure, were recorded every 2 seconds. Some of the speed and torque obtained in drilling experiment are shown in Figure 7. From the curve, it can find that the load applied on top drive shaft fluctuates randomly all time. And the pressure at outlet of hydraulic pumps varied with the load applied on the top drive. The pressure at the inlet of hydraulic pumps was remained at 1.57 MPa, which was the supplementary pressure of the system. As can be seen from Figure 7, the operating speeds of top drive were at 9 rpm, 11 rpm, 20 rpm, and 30 rpm, respectively. Though the output speed fluctuated randomly for the influence of load, the fluctuation was less than 2 rpm. In other words, at each running stage, the speed could be maintained at its setting value.

To verify and modify the mathematical model and simulation model built in this paper, a comparison analysis between the above three methods was performed. In

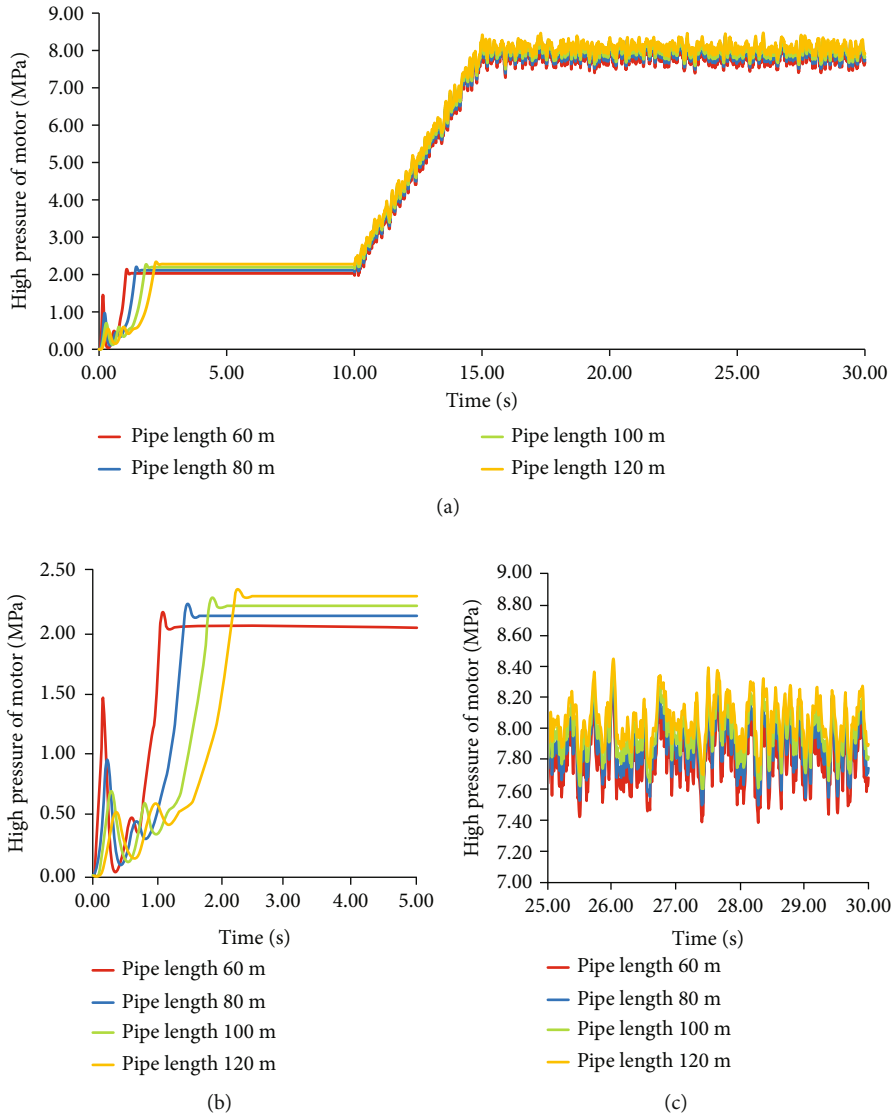

Figure 12: Hydraulic motor inlet pressure of the top drive with different pipe length. (a) Pressure from the beginning to the 30th second. (b) Pressure from the beginning to the 5th second. (c) Pressure from the 25th second to the 30th second.

the comparison, parameters of hydraulic pumps, hydraulic motors, and hydraulic pipelines were set at the same values for the three methods. Based on the measured torque of the field test, the load applied on the mathematical mode and simulation model is determined. From Figure 7, it can be found that it was not easy to find out the change rules of load on top drive and describe it with mathematical equations. So, a section of relative stable load was selected to be applied on the mathematical model and simulation model.

As shown in Figure 8, the blue curve represented the drilling experiment data measured in drilling experiment, the average value and fluctuation of which were 8000 N•m and 500 N•m, respectively. The green curve represented load applied on simulation model, and the purple curve represented the load applied on the mathematical model. Both the load applied on simulation model and mathematical model were divided into two stages. From the beginning to the third second, the system was in the state of no-load; from the third second to the end of the calculation, a random fluctuate torque was applied on the system, with an average value of 8000 N•m and fluctuating amplitude of 500 N•m.

Figure 9 shows the pressure difference of hydraulic motor obtained from the mathematical model, simulation model, and drilling experiment. From Figure 9, it could be found that, in the mathematical model, there was an overshoot of 6 MPa at the beginning stage of the system. Fluctuation of pressure losses decreased gradually, and the pressure loss reached to steady state in 0.5 second. In the simulation result, an overshoot of 1 MPa emerged at the beginning stage of simulation, and then the pressure difference of hydraulic motors oscillated with damping and reached to the steady state at 0.5 s. In the transient stage, the amplitude and

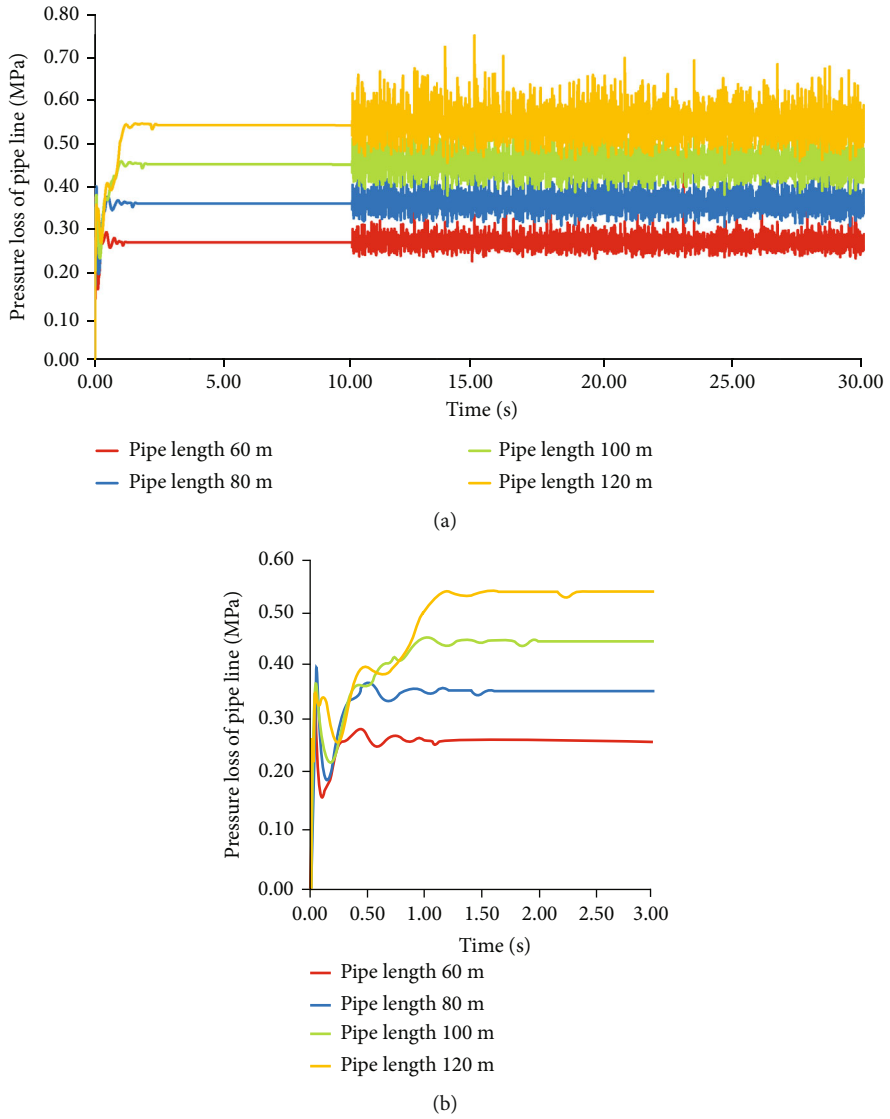

Figure 13: Pressure loss of the long pipelines with different length. (a) Pressure loss from the beginning to the 30th second. (b) Pressure loss from the beginning to the 3rd second.

frequency of vibration gained from mathematical model were both bigger than those gained from simulation model. At the 3rd second, the pipe pressure loss gained from mathematical model and simulation model both increased rapidly, with the overshoot of 7.51 MPa and 8.31 MPa, respectively. Then, the amplitude of pressure loss decreased, and the system reached to steady state within 1 second. The reason for the result difference between mathematical model and simulation model was that an approximate model derived from pipe four-ports distributed parameter model was used in mathematical model, while pipe lump parameter model was applied in simulation model.

When the system reached to steady state, the pressure loss of pipelines in mathematical model, simulation model, and drilling experiment all fluctuate with the load applied on hydraulic top drive shaft. In the mathematical model, the pressure loss changed around 5.51 MPa, with the fluctuation of 0.1 MPa; in simulation model, the pressure loss fluctuated around 5.85 MPa with the fluctuation of 0.2 MPa; in drilling experiment, the pressure loss fluctuated around 6.07 MPa with the fluctuation of 0.3 MPa. The cause of the difference in the steady-state output results of the above three methods was that several factors, the frictions of hydraulic motor and top drive shaft for example, are not considered in the mathematical model and simulation model.

Setting the speed of top drive at 30 rpm and applying loads as Figure 8 shown to the mathematical model and simulation model, the output speed is shown in Figure 10. The blue curve represented the speed measured in drilling experiment, the green cure represented the simulation results, and the purple curve represented the calculate results obtain from mathematical model. From the figure, it could be found that in the mathematical model, there was an overshoot of 52 rpm at the beginning of calculation, and then the system oscillated with

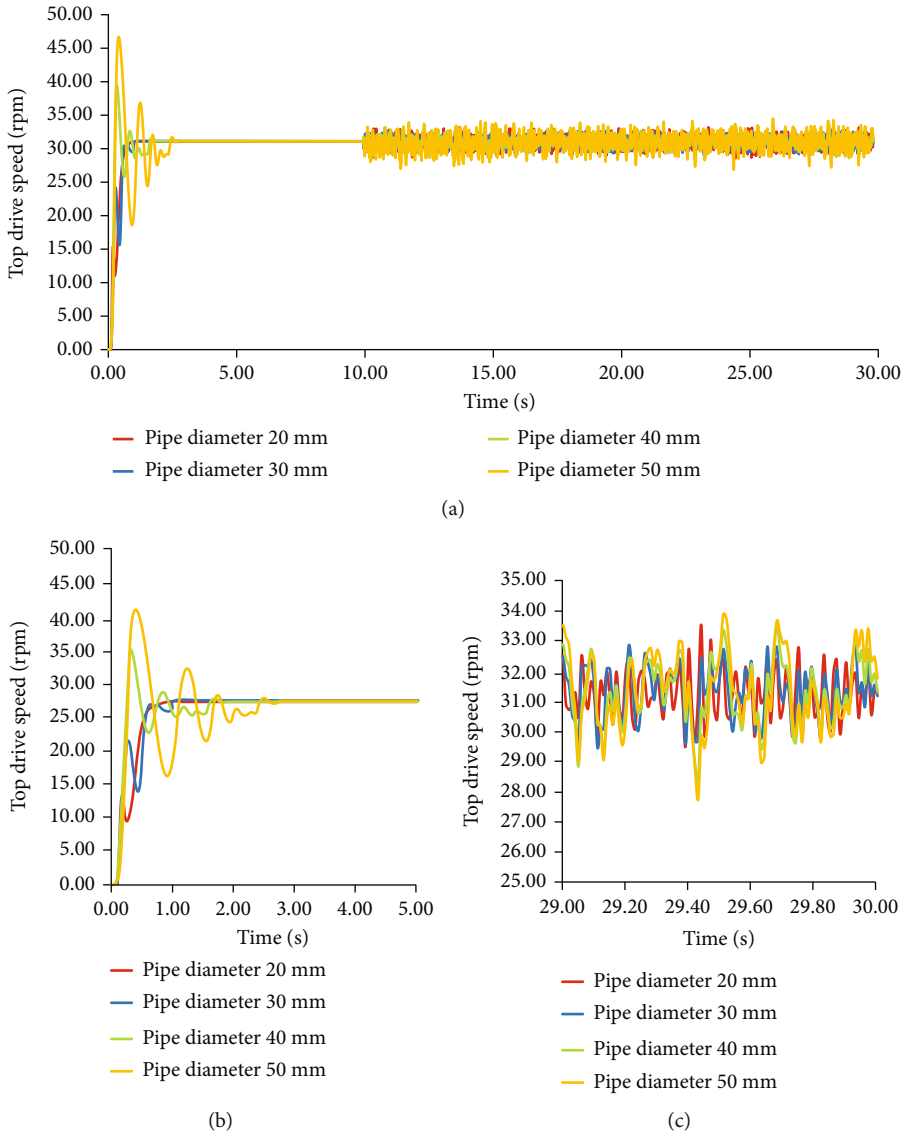

Figure 14: Top drive speed with different pipe diameter. (a) Speed from the beginning to the 30th second. (b) Speed from the beginning to the 5th second. (c) Speed from the 29th second to the 30th second.

fluctuation decreasing and reached to steady state within 1 second; at the 3rd second when load was began to be applied to the system, top drive speed dropped rapidly and then reached to steady state in 0.5 second. From the simulation result, it could be found that there was an overshoot of 7 rpm at the beginning of the simulation, and then the system oscillated with fluctuation decreasing and reached to steady state within 1 second; at the 3rd second when load was applied to the system, top drive speed dropped rapidly and then reached to steady state within 0.5 second. In the steady state, the mathematical result, simulation result and experiment result all fluctuated around 30 rpm, and the fluctuations were all less than 1 rpm. The results gained from the three methods coincided very well.

It can be seen from the comparative analysis that the mathematical model results, simulation results, and experimental data are basically consistent. The simulation model established in this paper can be used to study the dynamic characteristics of top drive with long hydraulic pipelines.

4.2. Output Characteristic of Hydraulic Top Drive with Different Hydraulic Pipe Length. When the set speed is 30 rpm and torque applied on the shaft is set to fluctuate between 7500 N•m and 8500 N•m, the output speed of top drive is shown in Figure 11 with the length of long pipelines of 50 m, 80 m, and 110 m, respectively. For clear observation of the dynamic response of the speed, Figure 11(b) and Figure 11(c) illustrate the top drive speed from the beginning to the 3rd second and from the 29th second to the 30th second, respectively. From the figure, it could be found that with the increase of the length of the pipelines, the responses of hydraulic top drive speed slowed down, and the overshoots decreased. When the system reached to steady state, the

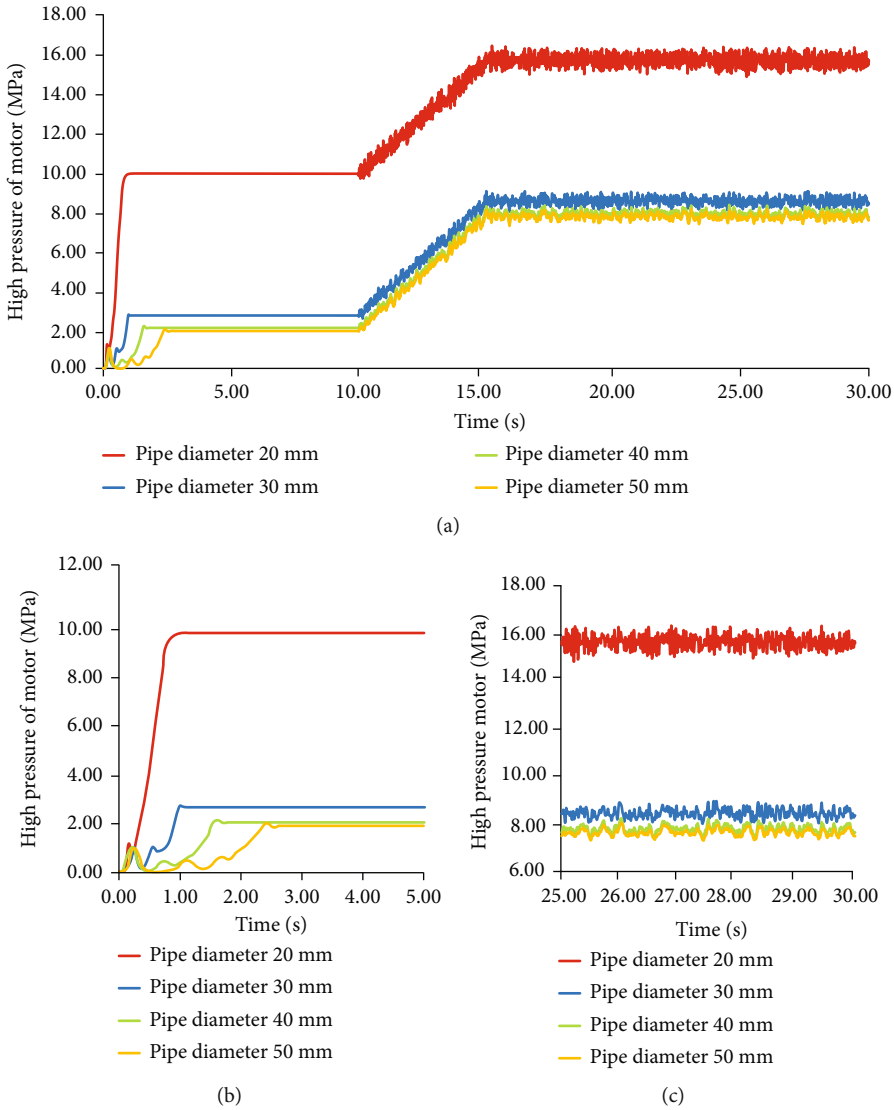

Figure 15: Hydraulic motor inlet pressure of the top drive with different pipe diameter. (a) Pressure from the beginning to the 30th second. (b) Pressure from the beginning to the 5th second. (c) Pressure from the 25th second to the 30th second.

steady-state value of hydraulic top drive speed fluctuated around the setting value of 30 rpm and the fluctuations increased with the length of pipelines increasing.

Figure 12 shows the inlet pressure of hydraulic motors. As can be seen from the figure, with the length of hydraulic pipelines increasing, fluctuations and the response speed of the pressure at the beginning decreased. When the system reached steady state, steady-state value of the pressure increased with the length of pipelines increasing, while the fluctuations decreased.

Figure 13 illustrates the pressure loss of high-pressure line of hydraulic top drive with different pipe length. It can be concluded from the plots that with the increase of hydraulic pipelines length, response of pressure loss slowed down. When the system reached to the steady state, the pressure loss and its fluctuation increased with the length of hydraulic pipeline increasing.

4.3. Output Characteristic of Hydraulic Top Drive with Different Pipe Diameters. When the setting speed of top drive was 30 rpm, and fluctuating load between 7500 N•m and 8500 N•m was applied on the top drive shaft, the output speed with different pipelines diameters is shown in Figure 14. From the figure, it could be found that with the increase of pipe diameter, the response of hydraulic top drive speed slowed down and the overshoot of hydraulic top drive speed increased. When the system reached to steady state, the hydraulic top drive speed fluctuated around the setting value of 30 rpm, but with the diameter of pipelines increasing, the fluctuation increased.

Figure 15 shows the inlet pressure of hydraulic motors with different diameters of hydraulic pipes. From the figure, it could be found that with the diameter decreasing, the fluctuation at the beginning decreased. When the system reached steady state, the steady-state value of inlet pressure

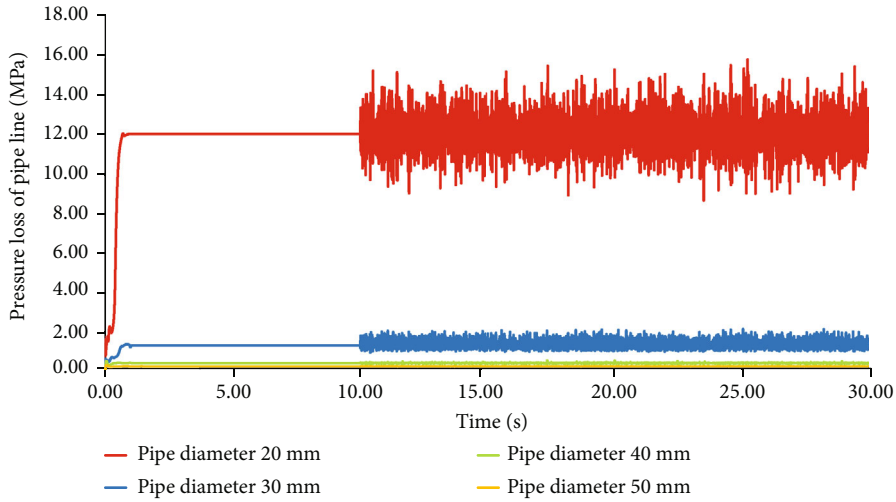

Figure 16: Pressure loss of the long hydraulic pipelines with different diameter.

and its fluctuation increased with the decrease of pipe diameters.

The pressure loss of hydraulic pipelines in high-pressure side with different diameters of hydraulic pipeline is shown in Figure 16. From the figure, it could be found that with the diameters decreasing, the pressure loss and its fluctuation both increased. When the diameters of hydraulic pipelines reached to 40 mm, the pressure loss would be very low.

5. Conclusions

Hydraulic top drive is mainly used to drive drilling tools rotating to drill a hole, whose main transmission system mainly consists of main gearbox, hydraulic system, and control system. For the hydraulic system, hydraulic variable displacement pumps are selected as the power units, and variable hydraulic displacement motors are chosen as the actuator units. In well site, the hydraulic power station is generally placed on the drilling floor or on the ground, while the body of hydraulic top drive is mounted on the derrick and travels up and down during drilling process. Thus, long hydraulic pipelines are needed to connect the hydraulic top drive and the hydraulic power station, which will influence the performance and dynamic characteristic of the hydraulic top drive. To study the dynamic performance, a mathematical model was developed by integrating the differential model of hydraulic units and approximate model of hydraulic pipelines. A simulation model based on the AMESim software was built. What's more, field drilling test of the hydraulic top drive was carried out in the Songliao Basin Drilling Project well site.

To verify and modify the mathematical model and simulation model built in this paper, a comparison analysis was performed by setting the parameters and load of the three methods at the same values. From the comparative analysis, it can be seen that the mathematical model results, simulation results, and experimental data are basically consistent. The simulation model established in this paper can be used to study the dynamic characteristics of top drive with long hydraulic pipelines.

Output characteristics of hydraulic top drive with different length and diameters of pipelines were studied in this paper. With the increase of the length of pipelines, the response speed of hydraulic top drive speed and the pressure loss in the high-pressure side pipelines slow down, while the response speed of hydraulic motor inlet pressure decreases at the beginning. When the system reaches to the steady state, the fluctuations of the hydraulic top drive speed and the pressure loss in the high-pressure side pipelines increase, while the fluctuations of the hydraulic motor inlet pressure decrease. As the diameters of hydraulic pipelines increase, the response of hydraulic top drive speed slows down, while the overshoot of hydraulic top drive speed and the fluctuations when the system reaches to steady state both increase. With increasing diameters, the steady-state value of inlet pressure and its fluctuation, the pressure loss of hydraulic pipelines in high-pressure side and its fluctuation both reduce.

Because the characteristics of hydraulic top drive speed and pressure output in very different laws with pipeline lengths and pipeline diameters change, it needs to comprehensively consider the system response speed, overshoot, and steady-state characteristics when choosing the size of pipelines for the hydraulic top drive. In order to reduce impacts of speed and pressure, the pipelines connecting hydraulic pumps and hydraulic motors would be not any longer than necessary.

Data Availability

The data used to support the findings of this study are available from the corresponding author upon request.

Conflicts of Interest

The authors declare that there are no conflicts of interest regarding the publication of this paper.

Acknowledgments

The research was funded by Natural Science Foundation of the Anhui Higher Education Institutions (KJ2019A0102), Natural Science Foundation of Anhui Province (2108085QE210), Major science and technology projects in Anhui Province (201903a05020012), and Scientific Research Foundation of AUST. The authors greatly appreciate the financial support from funding bodies.

References

[1] G. I. Boyadjieff, "An overview of top-drive drilling system applications and experiences," *SPE Drilling Enginerring*, vol. 1, no. 6, pp. 435–442, 1986.

[2] J. Pickett, J. Saski, R. Luher, A. Cantrell, and B. Wallihan, "The next generation top drive and lessons learned from the TDX-1250," in *SPE/IADC Drilling Conference and Exhibition*, Amsterdam, The Netherlands, 2011.

[3] Y. H. Sun, Y. L. Shi, Q. Y. Wang, and Z. W. Yao, "Study on speed characteristics of hydraulic top drive under fluctuating load," *Journal of Petroleum Science and Engineering*, vol. 167, pp. 277–286, 2018.

[4] S. Kumar, V. K. Tewari, C. K. Bharti, and A. Ranjan, "Modeling, simulation and experimental validation of flow rate of electro- hydraulic hitch control valve of agricultural tractor," *Flow Measurement and Instrumentation*, vol. 82, article 102070, 2021.

[5] X. Shang, H. Zhou, and H. Y. Yang, "Improving performance of a resonant string-based pulsation attenuator in hydraulic systems," *Applied Sciences*, vol. 10, no. 23, article 8526, 2020.

[6] R. Q. Ding, J. H. Zhang, B. Xu, M. Cheng, and M. Pan, "Energy efficiency improvement of heavy-load mobile hydraulic manipulator with electronically tunable operating modes," *Energy Conversion and Management*, vol. 188, pp. 447–461, 2019.

[7] W. U. Rehman, X. H. Wang, Y. Q. Cheng et al., "Motion synchronization for the SHA/EMA hybrid actuation system by using an optimization algorithm," *Automatika*, vol. 62, no. 3-4, pp. 503–512, 2021.

[8] W. Wu, C. F. Di, and J. B. Hu, "Dynamics of a hydraulic-transformer-controlled hydraulic motor system for automobiles," *Proceedings of the Institution of Mechanical Engineers Part D Journal of Automobile Engineering*, vol. 230, no. 2, pp. 229–239, 2016.

[9] C. G. Park, S. Yoo, H. Ahn, J. Kim, and D. Shin, "A coupled hydraulic and mechanical system simulation for hydraulic excavators," *Proceedings of the Institution of Mechanical Engineers, Part I: Journal of Systems and Control Engineering*, vol. 234, no. 4, pp. 527–549, 2020.

[10] D. X. Zhao, C. B. Xu, T. Ni, H. Y. Zhang, and R. B. Qiao, "Dynamic response and control accuracy optimization of marine hydraulic manipulator based on piecewise P and fuzzy PI control algorithms," *Journal of Intelligent & Fuzzy Systems*, vol. 38, no. 1, pp. 75–88, 2020.

[11] L. M. Yang and T. Moan, "Dynamic analysis of wave energy converter by incorporating the effect of hydraulic transmission lines," *Ocean Engineering*, vol. 38, no. 16, pp. 1849–1860, 2011.

[12] J. T. Karam and M. E. Franke, "The frequency response of pneumatic lines," *Journal of Basic Engineering*, vol. 89, no. 2, pp. 371–378, 1967.

[13] S. Tsao, "Numerical solutions of transients in pneumatic networks—transmission-line calculations," *Journal of Applied Mechanics*, vol. 35, no. 3, pp. 588–595, 1968.

[14] W. Liu, T. Wei, and Z. F. Yue, "Pressure pulsation analysis of aircraft hydraulic power pipelines system," *Advanced Materials Research*, vol. 97-101, no. 1662–8985, pp. 2861–2864, 2010.

[15] P. X. Gao, J. Y. Zhai, and Q. K. Han, "Dynamic response analysis of aero hydraulic pipeline system under pump fluid pressure fluctuation," *Proceedings of the Institution of Mechanical Engineers, Part G: Journal of Aerospace Engineering*, vol. 233, no. 5, pp. 1585–1595, 2019.

[16] P. X. Gao, T. Yu, Y. L. Zhang, J. Wang, and J. Y. Zhai, "Vibration analysis and control technologies of hydraulic pipeline system in aircraft: a review," *Chinese Journal of Aeronautics*, vol. 34, no. 4, pp. 83–114, 2021.

[17] W. Zhang, R. H. Shen, N. Xu, H. R. Zhang, and Y. T. Liang, "Study on optimization of active control schemes for considering transient processes in the case of pipeline leakage," *Energies*, vol. 13, no. 7, article 1692, 2020.

[18] N. Nedić, L. Dubonjić, and V. Filipović, "Design of constant gain controllers for the hydraulic control system with a long transmission line," *Forschung im Ingenieurwesen*, vol. 75, no. 4, pp. 231–242, 2011.

[19] L. Yang, J. Hals, and T. Moan, "Comparative study of bond graph models for hydraulic transmission lines with transient flow dynamics," *Journal of Dynamic Systems Measurement and Control*, vol. 134, no. 3, 2012.

[20] L. M. Yang and T. Moan, "Bond graph representations of hydraulic pipelines using normal modes with dissipative friction," *Simulation*, vol. 89, no. 2, pp. 199–212, 2013.

[21] W. C. Yang and W. E. Tobler, "Dissipative modal approximation of fluid transmission lines using linear friction model," *Journal of Dynamic Systems, Measurement, and Control*, vol. 113, no. 1, pp. 152–162, 1991.

[22] B. Ayalew and B. T. Kulakowski, "Modal approximation of distributed dynamics for a hydraulic transmission line with pressure input-flow rate output causality," *Journal of Dynamic Systems Measurement and Control*, vol. 127, no. 3, pp. 503–507, 2005.

[23] P. Casoli and A. Anthony, "Gray box modeling of an excavator's variable displacement hydraulic pump for fast simulation of excavation cycles," *Control Engineering Practice*, vol. 21, no. 4, pp. 483–494, 2013.

[24] G. Coskun, T. Kolcuoglu, T. Dogramacı, A. C. Turkmen, C. Celik, and H. S. Soyhan, "Analysis of a priority flow control valve with hydraulic system simulation model," *Journal of the Brazilian Society of Mechanical Sciences & Engineering*, vol. 39, no. 5, pp. 1597–1605, 2017.

[25] Y. Guo and R. He, "Design, modeling, and test: the hydraulic vibration energy recovery system of speed bump," *Journal of Energy Resources Technology*, vol. 142, no. 1, 2020.

[26] E. B. Wylie and V. L. Streeter, *Fluid Transients*, McGraw-Hill Book Company, New York, America, 1978.

[27] J. Sirohi, C. Cadou, and I. Chopra, "Investigation of the dynamic characteristics of a piezohydraulic actuator," *Journal of Intelligent Material Systems and Structures*, vol. 16, no. 6, pp. 481–492, 2005.